Available online at www.sciencedirect.com
SCIENCE DIRECT®
Nuclear Instruments and Methods in Physics Research A 558 (2006) 303–307
NUCLEAR INSTRUMENTS & METHODS IN PHYSICS RESEARCH Section A
www.elsevier.com/locate/nima

Simulation of crystalline beams in storage rings using molecular dynamics technique

I. Meshkov[a], T. Katayama[b], A. Sidorin[a], A. Smirnov[a,*], E. Syresin[a], G. Trubnikov[a], H. Tsutsui[b]

[a]*Joint Institute for Nuclear Research (JINR), Joliot Curie 6, Dubna 141980, Russian Federation*
[b]*Institute of Physical and Chemical Research (RIKEN), Hirosawa 2-1, Wako 351-0198, Japan*

Available online 28 November 2005

Abstract

Achieving very low temperatures in the beam rest frame can present new possibilities in accelerator physics. Increasing luminosity in the collider and in experiments with targets is a very important asset for investigating rare radioactive isotopes. The ordered state of circulating ion beams was observed at several storage rings: NAP-M [Budker, et al., in: Proceedings of the 4th All-Union Conference on Charged-Particle Accelerators [in Russian], vol. 2, Nauka, Moscow, 1975, p. 309; Budker et al., Part. Accel. 7 (1976) 197; Budker et al., At. Energ. 40 (1976) 49. E. Dementev, N. Dykansky, A. Medvedko et al., Prep. CERN/PS/AA 79-41, Geneva, 1979] (Novosibirsk), ESR [M. Steck et al., Phys. Rev. Lett. 77 (1996) 3803] and SIS [Hasse and Steck, Ordered ion beams, in: Proceeding of EPAC '2000] (Darmstadt), CRYRING [Danared et al., Observation of ordered ion beams in CRYRING, in: Proceeding of PAC '2001] (Stockholm) and PALLAS [Schramm et al., in: J.L. Duggan (Eds.), Proceedings of the Conference on Appl. of Acc. in Research and Industry AIP Conference Proceedings, p. 576 (to be published)] (Munich). In this report, the simulation of 1D crystalline beams with BETACOOL code is presented. The sudden reduction of momentum spread in the ESR experiment is described with this code. Simulation shows good agreement with experimental results and also with the intrabeam scattering (IBS) theory [Martini, Intrabeam scattering in the ACOOL-AA machines, CERN PS/84-9 AA, Geneva, 1984]. The code was used to calculate characteristics of the ordered state of ion beams for the TARN-II [Katayama, TARN II project, in: Proceedings of the IUCF workshop on nuclear physics with stored cooled beams, Spencer, IN, USA, 1984].
© 2005 Elsevier B.V. All rights reserved.

PACS: 29.27. Bd

Keywords: Electron cooling; Crystalline ion beams

1. Introduction

1.1. Motion equations

To calculate crystalline beams, pairs of canonical variables are chosen. Transverse motion is described by the traditional variables: coordinate and transverse momentum normalized on the longitudinal momentum. Longitudinal motion is defined as arrival time and longitudinal momentum as spread. The vector of canonical variables is as follows:

$$X = \left(x, p_x = \frac{P_X}{P_S},\ y,\ p_y = \frac{P_Y}{P_S},\right.$$
$$\left. z = -(t - t_0)\beta_0 c,\ p_z = \frac{E - E_0}{P_S \beta_0 c}\right), \quad (1)$$

where x, y are the horizontal and vertical positions, p_x, p_y are the corresponding normalized momenta, z is the arrival time of the particle times $-c\beta_0$, p_z is the normalized momentum spread $p_z = \Delta P/P_S$.

*Corresponding author. Tel.: +7 09621 564479; fax: +7 09621 65322.
E-mail address: smirnov@jinr.ru (A. Smirnov).

0168-9002/$ - see front matter © 2005 Elsevier B.V. All rights reserved.
doi:10.1016/j.nima.2005.11.028

A Hamiltonian for ordered state simulation is used with independent variable s:

$$H = -\frac{xp_z}{\rho} + \frac{p_z^2}{2\gamma_0^2} + \frac{p_x^2+p_y^2}{2} + \frac{1}{2}\left(\frac{1}{\rho^2}+K\right)x^2 - \frac{K}{2}y^2 + \frac{\lambda}{6}(x^3-3xy^2) + \frac{r_{\text{ion}}}{\gamma_0^2\beta_0^2}\sum_i \frac{1}{\sqrt{(x-x_i)^2+(y-y_i)^2+\gamma_0^2(z-z_i)^2}}, \quad (2)$$

where ρ is the curvature radius of the reference orbit. The effect of multipole components of the magnets is included with parameters K and λ, which are defined by

$$K \equiv \frac{1}{B\rho}\frac{\partial B_y}{\partial x}, \quad \lambda \equiv \frac{1}{B\rho}\frac{\partial^2 B_y}{\partial x^2}, \quad r_{\text{ion}} = \frac{Z^2}{A}\frac{e^2}{4\pi\varepsilon_0 m_u c^2}, \quad (3)$$

where $B\rho = p_0/q$ is the magnetic rigidity.

1.2. Molecular dynamics

The last element in Eq. (2) describes the Coulomb interaction between particles. Since the calculation of the space–charge effect is time consuming, a molecular dynamics (MD) technique, with periodic boundary condition, is used. When ions of charge $q = Ze$ are put at position $(s, r) = (0,0),(\pm L,0),(\pm 2L,0),\ldots$ (Fig. 1), the last element in the region $|s| < L/2$ is [1–8]

$$U_{\text{sc}}(s,r) = \frac{1}{4\pi\varepsilon_0}\left(\frac{q}{a} + \frac{2q}{L}\int_0^\infty \frac{J_0(kr/L)\cosh(ks/L)-1}{\exp(k)-1}\,\mathrm{d}k\right), \quad (4)$$

where q is particle charge, $a = \sqrt{s^2+r^2}$ is distance between particles, $s = z - z_i$, $r = \sqrt{(x-x_i)^2+(y-y_i)^2}$, L is MD cell size, J_0 is the Bessel function of 0th order. The space–charge force vector from the ith particle, with the MD technique, can be derived from Eq. (4)

$$F_{px} = \frac{1}{4\pi\varepsilon_0}\frac{q^2(x-x_i)}{m_0c^2\gamma_0^2\beta_0^2}\left(\frac{1}{a^3} - \frac{2I_1}{rL^2}\right),$$
$$F_{py} = \frac{1}{4\pi\varepsilon_0}\frac{q^2(y-y_i)}{m_0c^2\gamma_0^2\beta_0^2}\left(\frac{1}{a^3} - \frac{2I_1}{rL^2}\right),$$
$$F_{pz} = \frac{1}{4\pi\varepsilon_0}\frac{q^2(z-z_i)}{m_0c^2\gamma_0^2\beta_0^2}\left(\frac{1}{a^3} - \frac{2I_0}{sL^2}\right), \quad (5)$$

where

$$I_1 = -\int_0^\infty \frac{kJ_1(kr/L)\sinh(ks/L)-1}{\exp(k)-1}\,\mathrm{d}k,$$
$$I_0 = -\int_0^\infty \frac{kJ_0(kr/L)\cosh(ks/L)-1}{\exp(k)-1}\,\mathrm{d}k,$$

J_1 is the Bessel function of first order, m_0c^2 is ion rest mass. Integrals I_1 and I_0 were numerically calculated and are used in the program as table values. With this MD technique, the dynamics of the ordered state of ions in a storage ring is usually simulated with $N_{\text{p}} = 10/100$ particles.

1.3. Crystallization conditions

The main criterion for beam crystallization (orderliness) is a decrease in particle temperature, lower than inter-particle potential energy, which can be described by the plasma parameter:

$$\Gamma = \frac{U}{T} = \frac{1}{4\pi\varepsilon_0}\frac{Z^2e^2}{aT} > 1, \quad (6)$$

where U and T are potential energy and temperature of the ion beam, respectively. Ze is the charge of particles, a is average inter-particle distance. 3D crystals are obtained for plasma parameter $\Gamma \gg 150$.

The next condition is related to the optical structure of the storage ring. The storage ring must be alternating-gradient (AG) focusing and the beam energy must be less than the transition energy of the ring [9]:

$$\gamma < \gamma_{\text{T}}. \quad (7)$$

Another condition defines the periodicity of the ion storage ring. The ring lattice periodicity should be at least four times as high as the maximum betatron value [9]:

$$4\max\{Q_x, Q_y\} < \text{Periodicity}. \quad (8)$$

These conditions (Eqs. (6)–(8)) need to be satisfied for 3D crystalline beams. In the case of 1D ordered beam, other criteria were formulated [10]. The main criterion defines the situation where particles cannot pass each other in a longitudinal direction:

$$\Gamma_2 = \frac{1}{4\pi\varepsilon_0}\frac{Z^2e^2}{T_{\|}\sigma_\perp} > \pi, \quad (9)$$

where $T_{\|}$ is longitudinal temperature and $\sigma_\perp$ is transverse size of the ion beam. As will be shown below, the criterion Γ_2 plays a very important role in the process of beam ordering.

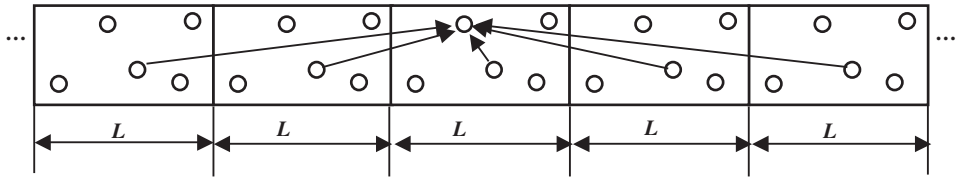

Fig. 1. Periodic distribution of five particles in MD cells.

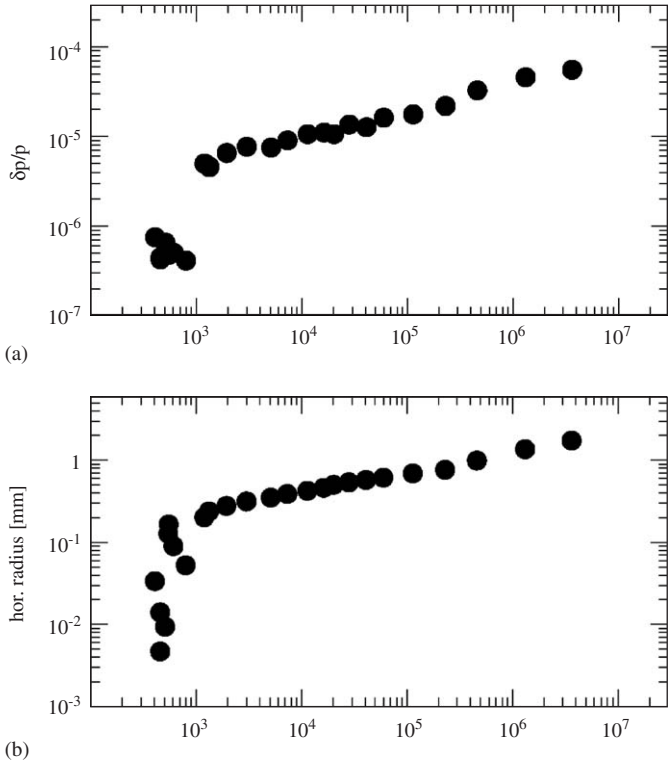

Fig. 2. Beam behavior in the ESR experiment showing the anomalous temperature reduction at low intensity. Momentum spread and beam size are given as functions of number of stored ions. $^{238}U^{92+}$ 400 MeV/u.

2. Ordered beams in storage rings

2.1. ESR experiments

Since the sudden reduction in momentum spread of a circulating proton beam was observed in NAP-M [1], the ordered state of ion beams has also been achieved on several storage rings. The most extensive experimental program was perfomed on the ESR [2]. The momentum spread reduction was observed for a wide range of ion species, except for very light ions.

On the ESR, the momentum spread of a uranium beam at 400 MeV/u, cooled by a 0.25 A electron beam, drops around 1000 stored ions, from a value of $\Delta p/p = 5 \times 10^{-6}$ to $\Delta p/p = 5 \times 10^{-7}$, corresponding to a change in longitudinal temperature of two orders of magnitude (Fig. 2) [11]. The scraper measurement allows derivation of the momentum spread and the beam radius as a function of the number of stored ions (Fig. 2). For the horizontal degree of freedom, a radius reduction from 0.2 mm to less than 0.01 mm is obvious. Despite the limited resolution, even for the vertical beam radius, a reduction is suggested by the data points at the transition point of the longitudinal momentum spread and the horizontal radius.

The behavior of ion beam values can be explained using 3D diagrams of beam parameter growth rates due to intrabeam scattering, which were calculated using a generalized Piwinski model [6]. The model presumes a sufficient number of particles and Gaussian distribution of the particles in all degrees of freedom. Horizontal and vertical emittances were chosen to be equal.

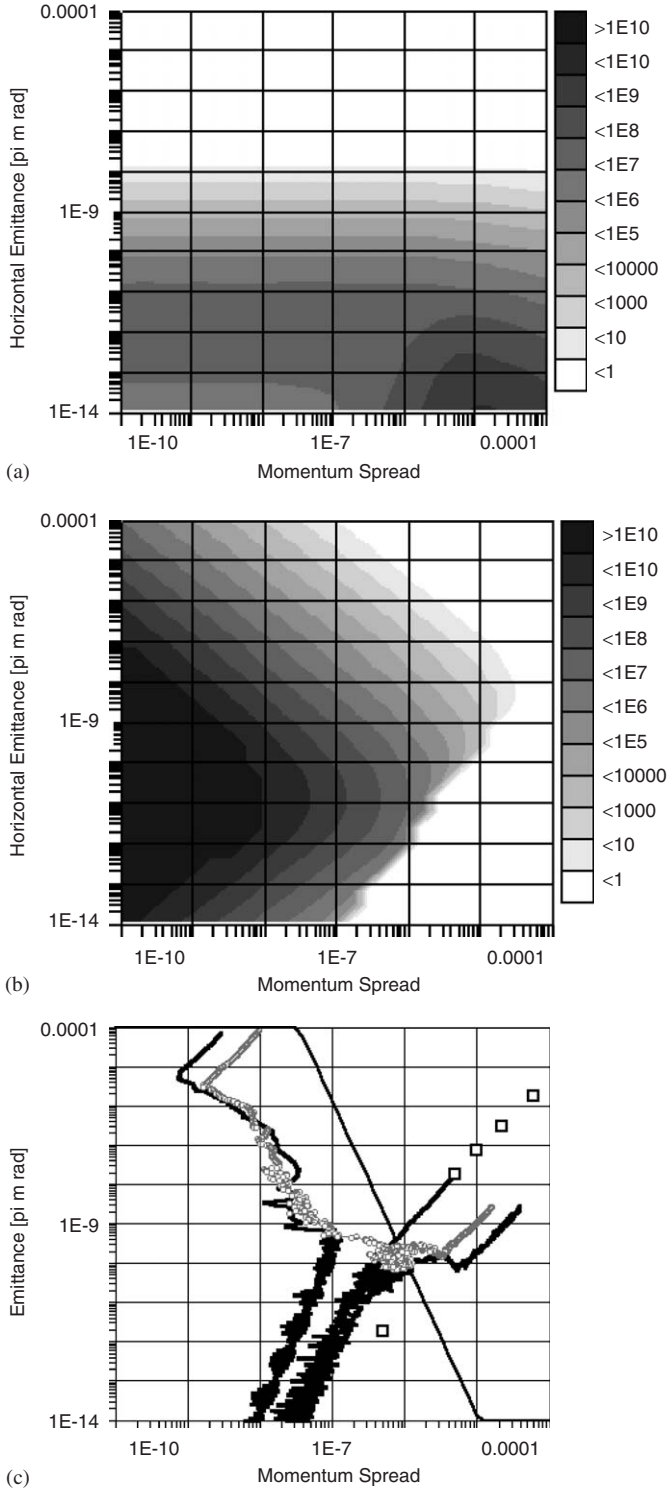

Fig. 3. Theoretical dependence of IBS growth rates on beam emittance and momentum spread for ESR: (a) horizontal and (b) longitudinal components of IBS growth rates. Results of MD calculations (c): evolution of ion beam parameters during cooling. Solid black line corresponds to cooling rate of 4×10^4 Hz. Grey circles correspond to cooling rate of 10^4 Hz. Straight line is criterion $\Gamma_2 = \pi$ ($N = 5 \times 10^5$). Open squares are ESR experiment (see Fig. 2).

The condition $\Gamma_2 = \pi$ (Eq. (9)) describes the following relationship between beam emittance and momentum spread: $\varepsilon \sim (\Delta p/p)^{-4}$. In the twice-logarithmic scale, this dependence is presented in Fig. 3(c) as a black solid line, where the theoretical dependence of intrabeam scattering (IBS) on beam values at high particle numbers is compared with the results of numerical simulation using the MD method [12]. In ESR experiments, the magnitude of beam emittances and momentum spread before momentum reduction are defined by equilibrium between IBS growth and cooling rates (series of square points on Fig. 3(c)). The experimental points lie on the line, which approximately corresponds to equal values of longitudinal and transverse growth rates. Particle numbers decrease with time and, when the Γ_2 value exceeds π, cooling forces suppress the IBS forces and the beam reaches an ordered state (last experimental point in Fig. 3(c)).

The calculated results, using the MD technique (Fig. 3(c)), are in good qualitative agreement with the 3D diagram (Figs. 3(a) and (b)). Calculations were performed using the same particle numbers, i.e. 5×10^{-5}, which is three orders of magnitude larger than in the ESR experiments. Cooling rates were also chosen as three orders larger, in comparison with real electron cooling systems. In the first stage of beam cooling, all the lines have the same angular inclination, determined by the ratio between cooling rates in transverse and longitudinal degrees of freedom. In the case of uniform cooling ($\varepsilon \sim (\Delta p/p)^2$), one can see this dependence in the initial part of the beam phase trajectory, independent of initial point. This means that at a large initial phase, space of the beam IBS process does not effect the cooling process.

Prior to the ordered state, MD calculations are in good agreement with the position of maximum IBS growth rates, as predicted by the Piwinski model. No other additional heating was used in these simulations. In the ordered state, IBS growth rates, calculated using the MD method, are substantially less than predicted by the Piwinski model. At a cooling rate of 4×10^4 Hz and higher, beam emittance and momentum spread decrease to very small values.

2.2. Simulation for TARN-II

The 3D phase diagrams of IBS heating rates, in accordance with the Martitni model for the TARN-II ring [7], display the same behavior as the ESR ring (Figs. 3(a) and (b)). To study intrabeam scattering in the ordered state, the 3D phase diagram of heating rates was numerically simulated using the MD technique. Initial distribution was generated with the same distance between particles in a longitudinal direction. Transverse emittance and momentum are generated with a Gaussian distribution. This means that particles initially have only kinetic energy in the longitudinal plane. Growth rates are calculated after a few hundred cycles, when relaxation between kinetic and potential energies in the longitudinal plane occurs. The solid black line in Fig. 4 corresponds to

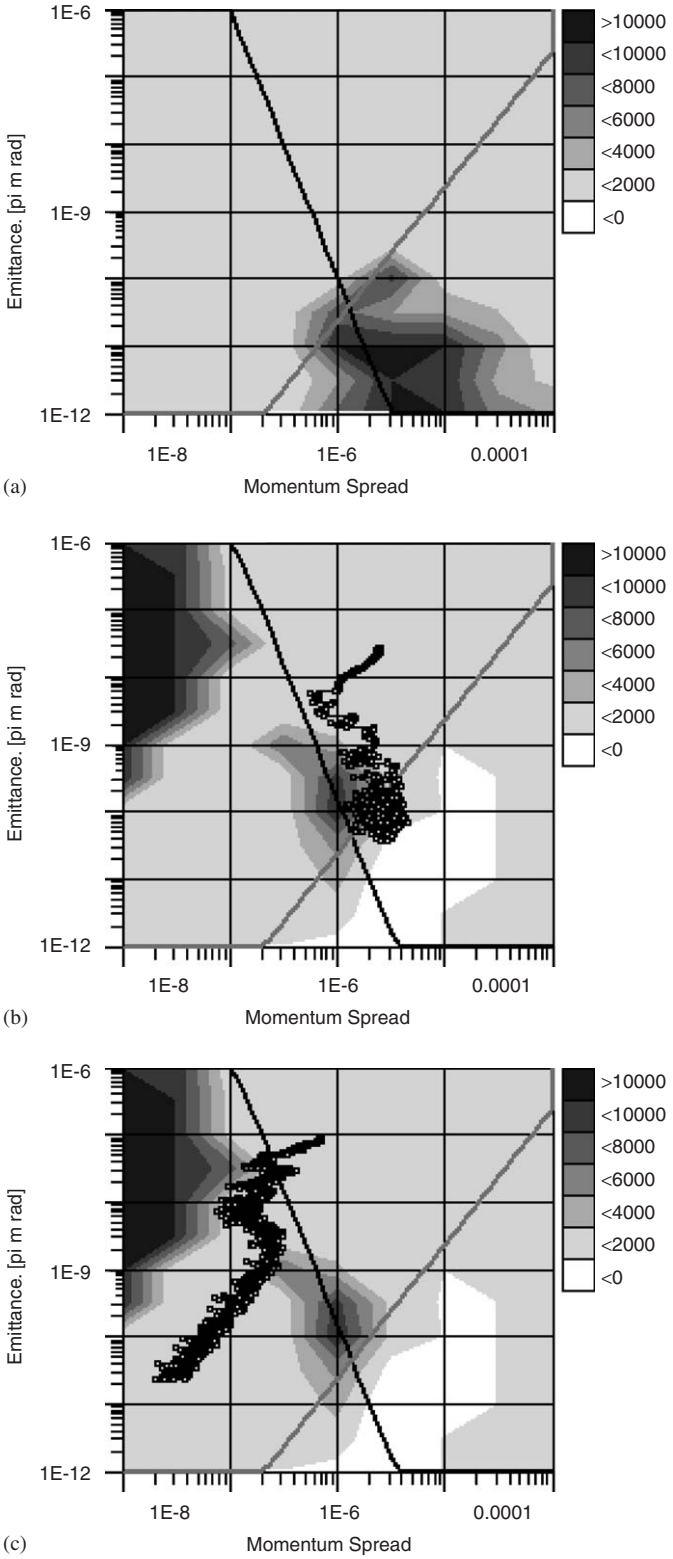

Fig. 4. MD simulation: (a) Horizontal component of IBS growth rates, (b) longitudinal component of IBS and (c) evolution of beam parameters during cooling process. $I_{ecool} = 5$ A, $^{132}Sn^{50+}$ 220 MeV/u, $N = 10^5$.

criterion $\Gamma_2 = \pi$; the gray line is the equilibrium between longitudinal and transverse temperatures. The intersection between criterion Γ_2 and temperature equilibrium is the final point before the sudden reduction of momentum

spread, which has been experimentally observed in a few storage rings.

The simulation result (Fig. 4) displays a number of differences from the theoretical model of IBS heating (Figs. 3(a) and (b)). Transverse components have very low heating rates for the range of momentum spread, which are located below the temperature equilibrium. Another big difference is the shape of the longitudinal component of IBS heating rate. It is divided into two parts. The first is defined by heating from an optic structure. The second part resembles an island whose height is linearly dependent on particle number and is well described by the IBS theory. The maximum of the IBS island is located near the intersection between criterion $\Gamma_2 = \pi$ and temperature equilibrium.

The longitudinal component of IBS heating breaks up when heating rates have very small values compared to the theoretical prediction. If the initial ion beam values are chosen near the break-up, then the ordered state for a large number of particle $N = 10^5$ can be achieved for a real cooling system with electron beam current $I_{\mathrm{ecool}} = 5\,\mathrm{A}$ (Fig. 4(c)).

To achieve ordered ion beams with a large number of particles and a realistic cooling force, a special strategy for the cooling process should be elaborated. When the ion beam remains in equilibrium between IBS and cooling, additional heating may be applied in the transverse direction. For example, heating by an RF-kicker can be used. Initially, the momentum spread will continue to decrease and emittances will increase. When the beam parameters have to satisfy the condition $T_\perp \gg T_\parallel$, the additional heating can be switched off and the ion beam will continue to cool down to the ordered state. The same idea is projected for other storage rings. Experimental verification of the new strategy for achieving an ordered ion beam with a large density can open new possibilities in accelerator physics.

3. Conclusion

Ion beam parameters, before momentum reduction, are defined by the equilibrium between cooling force and IBS. When cooling rate exceeds maximum IBS growth rate, the ion beam reaches an ordered state. The ESR case is studied in detail and simulation shows very good agreement with experimental results. Numerical simulation shows a large difference in the behavior of IBS heating in the ordered-state compared with the theoretical model. To increase particle numbers in the ordered state, a new strategy of cooling process is proposed. Additional heating in the transverse direction should be applied during the cooling process. For real cooling systems, the ordered state can be achieved with number of particles up to 10^5.

Acknowledgements

This work was supported by RFBR grant #02-02-16911, INTAS grant #03-54-5584.

References

[1] G.I. Budker, N.S. Dikansky, V.I. Kudelainen, et al., in: Proceedings of the Fourth All-Union Conference on Charged-Particle Accelerators [in Russian], vol. 2, Nauka, Moscow, 1975, p. 309;
G.I. Budker, N.S. Dikansky, V.I. Kudelainen, et al., Part. Accel. 7 (1976) 197;
G.I. Budker, N.S. Dikansky, V.I. Kudelainen, et al., At. Energy 40 (1976) 49;
E. Dementev, N. Dykansky, A. Medvedko, et al., Prep. CERN/PS/AA 79-41, Geneva, 1979.
[2] M. Steck, K. Beckert, H. Eickhoff, et al., Phys. Rev. Lett. 77 (1996) 3803.
[3] R.W. Hasse, M. Steck, Ordered ion beams, in: Proceeding of EPAC 2000.
[4] H. Danared, A. Kallberg, K.G. Rensfelt, A. Simonsson, Observation of ordered ion beams in CRYRING, in: Proceeding of PAC '2001.
[5] U. Schramm, T. Schätz, D. Habs, Laser-cooling of ions and ion acceleration in the RF-quadrupole ring trap PALLAS, in: J.L. Duggan (Ed.), Proccedings of the 16th International Conference on the Application of Accelerators in Research and Industry (CAARI), Denton, TX, USA, 11/2000, AIP Conference Procedings, 〈http:\\proceedings.aip.org/proceedings/confproceed/576.jsp〉 576, 667 (2001).
[6] M. Martini, Intrabeam scattering in the ACOOL-AA machines, CERN PS/84-9 AA, Geneva, 1984.
[7] T. Katayama, TARN II project, in: Proceedings of the IUCF Workshop on Nuclear Physics with Stored Cooled Beams, Spencer, IN, USA, 1984.
[8] V. Avilov, Solid State Commun. 44 (4) (1982) 555.
[9] J. Wei, A. Draeseke, M. Sessler, X. Li, Diverse topics in crystalline beams, in: Proceedings of the 31st Workshop of the INFN Eloisatron Project, Erice, Italy, 12–21 November 1995, p. 229.
[10] T. Katayama, I. Meshkov, A. Sidorin, A. Smirnov, E. Syresin, Ordered state of ion beams, Preprint RIKEN-AF-AC-40, 2002.
[11] M. Steck, K. Beckert, P. Beller, B. Franzke, F. Nolden, J. Phys. B 36 (2003) 991.
[12] T. Katayama, I. Meshkov, A. Sidorin, A. Smirnov, E. Syresin, H. Tsitsui, D. Mohl, Simulation study of ordered ion beams, Preprint RIKEN-AF-AC-42, 2003.